Spatial Regulation of Lck Activation at the Immune Synapse Revealed by a FRET-Based Biosensor

Clara Meana[1,3], Gonzalo San-José[1], María Beatriz Durán-Alonso[1,2], Javier Casas[1,2]

[1]Unidad de Excelencia Instituto de Biomedicina y Genética Molecular (IBGM), Consejo Superior de Investigaciones Científicas (CSIC) - Universidad de Valladolid (UVa), Spain

[2]Departamento de Bioquímica y Biología Molecular y Fisiología, Facultad de Medicina, Universidad de Valladolid, 47003 Valladolid, Spain

[3]Departamento de Pediatría e Inmunología, Universidad de Valladolid, Valladolid 47005, Spain

*** Correspondence:**
Corresponding Author
javier.casas@uva.es

Keywords: TCR, LCK, Immune Synapse, FRET, Spatial Regulation.

Abstract

T cell receptor (TCR) signaling is critically dependent on the Src-family kinase Lck, whose activation is tightly regulated both spatially and conformationally during antigen recognition. Here, we employ a third-generation FRET-based biosensor (TqLck-V2.3) to visualize Lck conformational dynamics in live T cells with high spatial resolution. Upon TCR engagement, we observe a paradoxical increase in whole-cell FRET signal, which immunolabeling reveals to be due to selective internalization of inactive Lck (pY505), while active Lck (pY394) remains membrane-associated and enriched at the immune synapse (IS). Using CD8α mutants that disrupt Lck binding, we demonstrate that free Lck undergoes more pronounced conformational activation than coreceptor-bound Lck. Furthermore, we show that C-terminal Src kinase (Csk) preferentially phosphorylates free Lck at Y505, while CD45 suppresses its activation via dephosphorylation of Y394, suggesting a dual regulatory mechanism that maintains free Lck in an inactive state under resting conditions. High-resolution imaging confirms sustained activation of Lck at the IS and transient inactivation at the periphery, revealing a spatially confined signaling architecture. These findings uncover a novel regulatory mechanism involving selective internalization and spatial segregation of Lck conformations and establish TqLck-V2.3 as a powerful tool for dissecting TCR signaling dynamics.

Introduction

T cell activation is a highly regulated process initiated by the engagement of the T cell receptor (TCR) with peptide–major histocompatibility complex (pMHC) molecules on antigen-presenting cells (APCs). This interaction triggers a cascade of intracellular signaling events, many of which are orchestrated by the Src-family kinase Lck. Lck plays a pivotal role in phosphorylating immunoreceptor tyrosine-based activation motifs (ITAMs) within the CD3 complex, thereby initiating downstream signaling pathways essential for T cell function and fate decisions.

Despite its central role, the mechanisms governing Lck activation and spatial regulation during TCR engagement remain incompletely understood. Lck exists in multiple conformational states, regulated by phosphorylation at two key tyrosine residues: Y394 (activating) and Y505 (inhibitory). The dynamic balance between these states is influenced by interactions with coreceptors (CD4/CD8), phosphatases, and kinases, as well as by the spatial organization of signaling complexes at the immune synapse.

Our previous work has proposed that free Lck, not bound to coreceptors, may be primarily responsible for initiating TCR signaling, while coreceptor-bound Lck contributes to signal amplification or stabilization. However, direct evidence supporting this model has been limited by the lack of tools capable of resolving Lck conformational changes in live cells with high spatial and temporal resolution. Current research indicates that in unstimulated T cells, the proportion of active Lck varies significantly, with studies reporting ranges from 2% to approximately 50% of the total Lck pool(1–3). This variation has inspired considerable debate in the field regarding the precise regulation and activation mechanisms of Lck(4).

Traditional approaches to studying Lck activation have relied heavily on biochemical methods such as Western blot and immunoprecipitation, which, while informative, cannot capture the spatial and temporal dynamics of Lck activation in living cells(2,3,5). Furthermore, technical challenges in sample preparation and antibody specificity have contributed to conflicting results in the literature(1,6). These limitations have highlighted the need for more sophisticated approaches to studying Lck regulation in situ.

Recent advances in fluorescence-based imaging techniques, particularly the development of FRET-based biosensors, have opened new possibilities for investigating the spatial and temporal aspects of Lck activation(7–9). These approaches allow for real-time monitoring of Lck conformational changes and activation states within the complex environment of the immune synapse, providing unprecedented insight into the spatial regulation of TCR signaling machinery.

We used a third-generation FRET-based biosensor, TqLck-V2.3, optimized for monitoring Lck conformational dynamics in T cells. Ratiometric FRET enables real-time monitoring of dynamic molecular interactions with high temporal resolution, which is critical for capturing the fast kinetics of early T cell signaling events. Unlike Fluorescence Lifetime Imaging Microscopy (FLIM), which requires longer acquisition times and complex data fitting to resolve fluorescence lifetimes, ratiometric FRET can be implemented with standard widefield or confocal microscopy, allowing for faster image

acquisition and analysis. This speed is essential for studying transient signaling intermediates and spatially localized activation patterns at the immunological synapse. TqLck-V2.3 enables the visualization of Lck conformational states in live T cells and provides insights into the spatial compartmentalization of active and inactive Lck during immune synapse formation. In this study, we combine live-cell imaging, phospho-specific labeling, and mutant T cell models to dissect the conformational regulation of Lck during antigen recognition. Our findings reveal a novel mechanism of Lck regulation involving the selective internalization of its inactive form and demonstrate that free Lck undergoes more substantial conformational changes than coreceptor-bound Lck upon TCR engagement

Material & Methods

2.1 Constructs and cells.

CHO cells expressing the tetracycline repressor (Thermo TRex) under blasticidin selection (10 μg/ml) were grown in Ham's F12 media with 10% (vol/vol) FCS, 100 U/ml of penicillin, 10 mg/ml of streptomycin, hygromycin 0.3 mg/ml and G418 0.8 mg/ml. Hybridomas expressing the OT-I TCR with or without CD8α and CD8β were made by retroviral transfection of TCR-deficient 58α-β cells (10). The plasmid pEF-TqLckV2.3 was provided by Dr. Burkhart Schraven from Magdeburg University. TqLckV2.3 was amplified by PCR adding 5´Hind-III and Not-I 3´specific restriction sites and inserted into retroviral vector pBMN-Z (S. Kinoshita and G. Nolan, www.stanford.edu/group/nolan). All the mutants were made using the Quickchange Site Mutagenesis Kit (Stratagene). Supernatants of these cells were used to transduce OT-I hybridomas. OT-I hybridoma cells were maintained in IMDM medium containing 10% fetal bovine serum, 2 mM L-glutamine, 100 U/ml penicillin/streptomycin, 50 μM β-mercaptoethanol,500 μg/ml G418 (selecting for TCRα) and 3 μg/ml puromycin (selecting for TCRβ).

pHR-Csk-P2A-Cbp and pHCM-mCherry-CD45cytCD43ex were kindly provided by Dr. John James from Oxford University.

2.2 Flow cytometry.

All flow cytometry was conducted on Cytek Aurora cytometer at the Institute of Biomedicine and Molecular Genetics flow cytometry facility. Flow cytometry data were analyzed in FlowJo (Tree Star) and exported where necessary.

2.3 Lentiviral and retroviral Transduction

VSV-G–pseudotyped lentiviral particles were produced by co-transfection of 293FT cells with transfer constructs (CD45cyt-CD43ex and Csk-P2A-Cbp) and the compatible packaging plasmids pMD2.G and psPAX2 in the presence of PEI 25K. Ecotropic retroviral particles were produced by co-transfection of Plat-E cells with transfer constructs (pBMN-TqLckV2.3, pBMN-CD8α-CxCP or pBMN-CD8β) and the compatible packaging plasmid pCL-Eco in the presence of PEI 25K. Viruses were harvested at 48 and 72 hours after transfection. Viral transduction of OT-I T cell hybridomas were carried out using concentrated viral particles in the presence of 8 μg/ml Polybrene (Sigma-

Aldrich), and infected cells were selected by FACS sorting or antibiotic resistance and subjected to imaging experiments.

2.4 Live Cell FRET Imaging

A dual superfast external excitation/emission wheels specifically designed for FRET were used for imaging, allowing almost simultaneous acquisition of donor and acceptor emission during donor excitation (20 ms delay). This consisted in a Leica K5 sCMOS camera attached to a Leica Dmi8 inverted microscope equipped with aforementioned ultrafast external filter wheels and a CoolLED 3 illumination system. Cells expressing Lck activity FRET-based sensor (TqLckV2.3) were cultured in glass-bottomed culture dishes (Mat-Tek). When improved adhesion was required, the glass was coated with poly-L-lysine (Sigma). The culture medium was replaced with HBSS supplemented with 10 mM HEPES, pH 7.4, 1.3 mM $CaCl_2$, and 1.3 mM $MgCl_2$. Cells were visualized at 37°C using a Leica Dmi8 system with an HC PL FLUOTAR 63X/1.3 NA oil immersion lens and an infrared focus maintenance system. Proper localization of the sensor was confirmed by obtaining YFP images. For ratiometric imaging, Turquoise (Tq) fluorescence was obtained using an excitation filter at 430/24 nm and an emission filter at 470/24 nm, Venus using an excitation filter at 500/20 nm and an emission filter at 535/30 nm, and FRET, without correction, using the Tq excitation filter at 430/24 nm and the Venus emission filter. The acquisition of the three channels was virtually simultaneous. We recorded a 2 min baseline before adding T cells acquiring images each 5 s. ImageJ software with custom plugins was used to correct both the movement and the background of the raw images and to create pixel-by-pixel FRET/Tq ratio images.

2.5 Immunocytochemistry Analyses

For phospho-specific staining of Lck, cells were fixed with 4% paraformaldehyde for 20 min in suspension and then permeabilized with 0.1% Triton X-100 for 20 min at room temperature. Cells were treated with 5% goat serum for 30 min and incubated with antibodies against phospho Y505, phospho Y394, total Lck (Cell Signaling) or phospho-Tyr (4G10 clone, Merck) for 1h. After washing, the cells were incubated with spectrally appropriate Alexa Fluor-conjugated Fab fragments against primary species antibodies (Thermo) for 1h. After intracellular staining, nuclei were counterstained with the DNA binding dye Hoechst 33342 (Thermo). All images were captured with a Leica confocal system TCS SP5X inverted microscope with a HCS Plan Apo CS 63X/1.4 NA oil immersion lens. Leica Application Suite Advanced Fluorescence software was used for the capture, and ImageJ was used for deconvolution (Parallel Iterative 3D plugin), image presentation and quantification.

Results

3.1 Functionality of a third-generation FRET-based Lck biosensor

To monitor Lck conformational dynamics in live cells, we employed an optimizedand based on second-generation FRET-based biosensor, TqLck-V2.3. In this construct, the original CFP and YFP fluorophores were replaced with monomeric Turquoise2 (Tq) and monomeric Venus (V), respectively(7) . Additionally, the entire insert was codon-optimized to minimize recombination events during retroviral cloning. Importantly, the donor fluorophore (Tq) was repositioned between the SH3

152 and SH2 domains of Lck, based on prior findings by Paster et al. demonstrating that this configuration
153 (as in CLck-Y2) more accurately recapitulates TCR-mediated signaling compared to other biosensor
154 designs (Fig. 1A)(11).

155 We first confirmed the biosensor's localization by confocal microscopy, validating its predominant
156 presence at the plasma membrane and exclusion from the cytoplasm (Fig. 1B). Upon treatment with
157 the Lck inhibitor PP2, we observed an increase in the FRET/Tq ratio, consistent with a closed (inactive)
158 Lck conformation. Conversely, stimulation with pervanadate, a phosphatase inhibitor that mimics TCR
159 activation, led to a decrease in the FRET/Tq ratio, indicative of an open (active) conformation (Fig.
160 1C). Notably, unstimulated cells exhibited a broad distribution of FRET/Tq ratios, likely reflecting the
161 presence of distinct Lck pools in different conformational states.

162 **3.2 Quantitative Analysis of Lck Regulation via TCR–pMHC Conjugate Formation in antigen**
163 **presenting surfaces**

164 To investigate Lck regulation in the context of antigen presentation, we developed an improved assay
165 system tailored to measure T-cell receptor (TCR) engagement with peptide–MHC (pMHC) complexes.
166 The OT-I TCR recognizes the OVA peptide (SIINFEKL) with high affinity when presented by H-2Kb,
167 but does not respond to the VSV peptide (RGYVYQGL) in the same context. Specifically, we analyzed
168 conjugate formation between OT-I cells expressing CD8α and CD8β (hereafter referred to as OT-
169 I.WT) and a surrogate antigen-presenting cell line. We used CHO cells engineered to express
170 doxycycline (DOX) inducible single-chain H-2Kb molecules constitutively loaded with either the
171 agonist peptide OVA (scH-2Kb–OVA) or the non-stimulatory peptide VSV (scH-2Kb–VSV), as
172 previously described (12,13) (Fig. 2A, B). To generate stable and functional single-chain pMHCI (sc-
173 pMHCI) molecules, we employed recombinant constructs in which the MHC-binding peptide was
174 fused to the N-terminus of β2-microglobulin, followed by linkage to the N-terminus of the MHCI
175 heavy chain, as previously described(14–16). When expressed on the cell surface, these constructs
176 exhibited high stability and effectively triggered T cell activation.

177 Quantification of conjugate formation revealed a time-dependent increase in the percentage of OT-
178 I.WT cells forming conjugates with CHO cells upon induction of pMHC expression. This increase was
179 significantly greater when CHO cells presented the antigenic OVA peptide compared to the non-
180 antigenic VSV peptide. In the absence of doxycycline (repressed state), there was some "leaky"
181 expression of sc-KbOVA, which was sufficient to trigger partial CD69 upregulation in CD8 OT-I T
182 cells, however, this level of expression did not lead to significant TCR downregulation (12,13) . Flow
183 cytometry using a KbOVA-specific antibody revealed that sc-KbOVA expression under these
184 conditions was nearly undetectable.

185 To assess early T-cell activation, we measured global tyrosine phosphorylation levels after 15 minutes
186 of co-culture using phospho-tyrosine staining (Fig. 2C). OT-I.WT cells exposed to CHO cells
187 presenting Kb:OVA exhibited elevated phospho-tyrosine levels relative to those exposed to Kb:VSV.
188 Pre-treatment of OT-I.WT cells with either a TCR-blocking antibody or the Src-family kinase inhibitor
189 PP2 abrogated this phosphorylation response, reducing it to levels comparable to those observed with
190 the non-stimulatory VSV peptide (Fig. 2C). Together, these results demonstrate that OT-I.WT T cells
191 selectively form stable conjugates and initiate early activation signaling in response to antigenic pMHC
192 complexes, highlighting the specificity and functional sensitivity of TCR–pMHC interactions in this
193 system.

194 **3.3 Validation of a third-generation FRET-based Lck biosensor for live-cell imaging**

195 Having validated the TqLck-V2.3 biosensor for monitoring Lck conformational changes, we next
196 employed confocal microscopy to assess Lck dynamics in a more spatially resolved context. OT-I T
197 cells expressing the biosensor were seeded onto monolayers of CHO cells inducibly expressing pMHC
198 complexes. Z-projection imaging was used to capture the full three-dimensional interaction interface
199 between T cells and the CHO monolayer as shown in Fig. 2D.

200 Unexpectedly, when CHO cells presented the antigenic OVA peptide, we observed a significant
201 increase in the FRET/Tq ratio across the entire T cell (Fig. 2E), suggesting a shift toward a closed
202 (inactive) Lck conformation. To investigate this paradoxical finding, we performed immunolabeling
203 using phospho-specific antibodies targeting Lck phosphorylated at Y394 (active form) and Y505
204 (inactive form).

205 Immunofluorescence analysis revealed that following TCR engagement, active Lck (pY394) remained
206 localized at the plasma membrane, whereas the inactive form (pY505) was predominantly internalized
207 (Fig 3A). These results support the FRET-based observation of increased closed conformation when
208 analyzing the whole cell and suggest that internalization of inactive Lck contributes to the overall
209 FRET signal, while active Lck remains membrane-associated. The selective internalization of Y505-
210 phosphorylated (inactive) Lck following TCR engagement suggests a previously unrecognized
211 regulatory mechanism that may spatially restrict Lck activity by compartmentalizing its inactive pool
212 away from the site of TCR stimulation, normally the immune synapse. Altogether, these findings
213 establish TqLck-V2.3 as a powerful biosensor for dissecting Lck conformational dynamics in live cells
214 and uncover a novel mechanism of spatial regulation whereby inactive Lck is selectively internalized
215 following TCR engagement, potentially fine-tuning signaling at the immune synapse.

216 **3.4 Lck biosensor reveals conformational activation at the immune synapse upon TCR**
217 **engagement and distinguishes coreceptor independent Lck pools**

218 To investigate the spatial and conformational dynamics of Lck activation during T-cell receptor (TCR)
219 engagement we used fast FRET live cell microscopy. Stimulation with crosslinking biotinylated
220 αCD3/αCD8 antibodies induced a 5 minute decrease in the FRET/Tq ratio as shown in Fig. 4A. This
221 conformational change was abolished by PP2 pre-treatment, confirming that the observed FRET signal
222 corresponds to Lck activation. To assess the biosensor's performance in a more physiological context,
223 we co-cultured TqLck-V2.3-expressing OT-I T cells with CHO cells presenting either scH-2Kb–OVA
224 or scH-2Kb–VSV and monitored FRET changes at the immune synapse. A significant decrease in the
225 FRET/Tq ratio was observed only in response to OVA presentation, indicating Lck activation in the
226 immune synapse upon antigen recognition (Fig. 4B).

227 Previous results indicated that free Lck is initially responsible for TCR triggering (17). To further
228 dissect the contribution of coreceptor-bound versus free Lck, we expressed the TqLck-V2.3 biosensor
229 in OT-I T cells carrying a mutation in the intracellular CxCP motif of CD8α (C227K/C229P mutated
230 to S227K/S229P), which disrupts Lck binding (17). This is hereafter referred to as OT-I.CxCP.
231 Interestingly, these mutant cells exhibited a more pronounced FRET/Tq ratio decrease upon OVA
232 recognition compared to wild-type cells, suggesting that free Lck undergoes more substantial
233 conformational changes than coreceptor-bound Lck during TCR engagement (Fig. 4C). These results
234 align with previous findings that initial TCR triggering is mediated predominantly by free Lck rather
235 than coreceptor-bound Lck (17).To further investigate the spatial dynamics of free Lck during antigen
236 presentation, we manually quantified FRET efficiency of the Tq-LckV2.3 biosensor at the IS and
237 across the remaining plasma membrane (Fig. 4D). During the initial phase of T cell–APC contact (0–
238 60 s), we observed a marked decrease in FRET signal at the IS, indicative of sensor opening and most

239 likely a higher Lck activity. In contrast, an increase in FRET was detected in the rest of the membrane,
240 suggesting Lck inactivation in those regions. In the subsequent 60 seconds, the sensor at the rest of the
241 membrane exhibited a closure, consistent with increased Lck activity, which remained stable
242 throughout the rest of the interaction. Notably, the previously opened sensor in IS regions maintained
243 its conformation (Fig. 4D), indicating a sustained spatial segregation of Lck activity during the T cell–
244 APC engagement.

245

246

247

248 **3.5 High-Resolution Imaging Reveals Spatial Restriction of Active Lck at the Immune Synapse**

249 Since free Lck seems to be responsible for initial TCR triggering, to enhance spatial resolution and
250 better characterize Lck conformational dynamics at the immune synapse (IS), we performed
251 deconvolution confocal microscopy on fixed cells. Fig. 4E shows a representative conjugate between
252 an OT-I CxCP mutant T cell expressing the TqLck-V2.3 biosensor, where Lck can´t bind to coreceptor,
253 and a Cy5-labeled CHO antigen-presenting cell expressing Kb-OVA (Fig. 4E) or Kb-VSV (Fig. 4F).

254 FRET/Tq ratio imaging revealed a distinct decrease in the ratio at the IS upon recognition of Kb-OVA
255 (but not Kb-VSV), indicating the presence of Lck in an open (active) conformation upon cognate
256 antigen recognition. Notably, a subtle but consistent increase in the FRET/Tq ratio was observed at the
257 periphery of the IS. This is consistent with the elevated FRET/Tq levels previously detected in the non-
258 synaptic membrane regions by live-cell fluorescence microscopy (Fig. 4D). This spatial pattern
259 suggests that only the open conformation of Lck is selectively enriched within the synapse, while the
260 closed (inactive) form may be excluded or retained at the borders.

261 **3.6 Csk preferentially phosphorylates Lck not bound to coreceptors**

262 To establish a latent system where we can distinguish the role of spatial conformation of free Lck and
263 coreceptor bound Lck, we next sought to restrain the kinase activity of Lck by overexpressing C-
264 terminal Src kinase (Csk). Csk is a key negative regulator of Lck, phosphorylating its inhibitory
265 tyrosine residue (Y505) to promote a closed, inactive conformation. This phosphorylation event
266 counterbalances the activating phosphorylation at Y394, thereby modulating Lck catalytic activity.
267 Importantly, Csk lacks intrinsic membrane-targeting domains and relies on adaptor proteins such as
268 PAG/Cbp to localize to the plasma membrane, where it can access Lck. To investigate whether Csk
269 preferentially phosphorylates coreceptor-bound or free Lck, we expressed the FRET-based Lck activity
270 sensor Tq-LckV2.3, along with Csk and Cbp, in OT-I T cells co-expressing either wild-type CD8α or
271 a CxCP mutant that disrupts Lck–coreceptor interaction. In cells expressing the CxCP mutant, we
272 observed a marked increase in the FRET/Tq ratio of the Lck sensor when Csk and Cbp were co-
273 expressed, indicative of a closed Lck conformation and consistent with enhanced phosphorylation at
274 the inhibitory Y505 site (Fig. 5). These results suggest that Csk preferentially targets coreceptor-free
275 Lck for inhibitory phosphorylation.

276 **3.7 CD45 Suppresses Free Lck Activation via Tyr394 Dephosphorylation to Prevent Spontaneous**
277 **TCR Signaling**

278 CD45 is a tyrosine phosphatase that modulates T cell signaling in a complex manner by
279 dephosphorylating both the inhibitory Tyr505 and the activating Tyr394 of Lck, thereby exerting both
280 activating and suppressive control depending on the context and localization of Lck. To investigate the
281 regulatory role of CD45 on distinct pools of Lck in resting T cells, we examined the conformational
282 changes in free (non coreceptor-bound) Lck. We made use of the construct CD45cytCD43ex-mCherry
283 (18,19) where the cytoplasmic phosphatase domains of CD45 were fused to the large extracellular and
284 transmembrane domains of CD43. Although CD43 ectodomain shares no amino acid similarity with
285 CD45, it is as long and as heavily glycosylated as that of CD45 and should therefore mimic its basic
286 physicochemical properties. This construct has previously been shown to functionally replicate
287 CD45(18). We used the TqLckV-2.3 biosensor in the presence or absence of CD45cytCD43ex-
288 mCherry in resting cells, We observed a consistent FRET increase in the free Lck pool when
289 CD45cytCD43ex-mCherry was expressed in CD8α-CxCP mutant expressing cells (Fig. 5). This
290 suggests that CD45 preferentially targets Tyr394 in free Lck, in contrast to its well-characterized role
291 in dephosphorylating the inhibitory Tyr505 site as shown when Lck can be also bound to CD8
292 coreceptor (Fig. 5). These findings imply that CD45 may act as a negative regulator of free Lck by
293 maintaining it in an inactive state through dephosphorylation of the activating site. This observation
294 suggests that CD45 actively suppresses the activation of free Lck by targeting its activating
295 phosphorylation site. It further suggests that CD45 functions as a gatekeeper, maintaining free Lck in
296 an inactive state under resting conditions. This mechanism may serve to prevent spontaneous or ligand-
297 independent TCR triggering, ensuring that T cell activation is tightly regulated and spatially restricted
298 to appropriate signaling contexts.

299 **4. Discussion**

300 T cell activation is a tightly regulated process that relies on the precise spatial and temporal
301 coordination of signaling molecules at the immune synapse. Among these, the Src-family kinase Lck
302 plays a pivotal role in initiating TCR signaling by phosphorylating ITAMs within the CD3 complex.
303 While the importance of Lck is well established, the mechanisms that regulate its activation and
304 localization during antigen recognition remain incompletely understood. In this study, we employed a
305 third-generation FRET-based biosensor, TqLck-V2.3, to visualize Lck conformational dynamics in
306 live T cells and dissect the contributions of coreceptor-bound versus free Lck during TCR engagement.

307 TqLck-V2.3 biosensor reports on the conformational state of Lck but does not differentiate between
308 the primed (open, non-phosphorylated) and double-phosphorylated (open, phosphorylated at both
309 Tyr394 and Tyr505) forms, as both adopt a constitutively open conformation that is insensitive to TCR
310 stimulation(7,8) . Latest studies show that the proportion of active Lck in resting T cells might be as
311 low as 2% of the total Lck population (1) therefore, any conformational opening changes detected by
312 the biosensor upon TCR engagement are likely indicative of Lck activation events.

313 Our results demonstrate that Lck undergoes distinct conformational changes upon TCR stimulation,
314 with a rapid decrease in the FRET/Tq ratio indicating a transition to an open, active conformation. This
315 activation was abrogated by the Src-family kinase inhibitor PP2, confirming the specificity of the
316 biosensor for Lck activity. Importantly, we observed that antigen-specific stimulation with CHO cells
317 presenting OVA-loaded pMHC induced a robust FRET response, whereas non-stimulatory VSV-
318 loaded pMHC did not, validating the biosensor's sensitivity to physiologically relevant TCR signals.

319 Unexpectedly, whole-cell imaging revealed an increase in the FRET/Tq ratio upon antigen recognition,
320 suggesting a paradoxical shift toward a closed Lck conformation. Immunofluorescence analysis
321 resolved this discrepancy by showing that inactive Lck (pY505) is selectively internalized following

322 TCR engagement, while active Lck (pY394) remains at the plasma membrane. This spatial segregation
323 implies a novel regulatory mechanism in which the internalization of inactive Lck may serve to sharpen
324 the signaling interface by restricting kinase activity to the immune synapse.

325 Further, our use of a CD8α mutant that disrupts Lck binding revealed that free Lck undergoes more
326 substantial conformational activation than coreceptor-bound Lck. This finding supports previous
327 models suggesting that free Lck is primarily responsible for initiating TCR signaling, while coreceptor-
328 bound Lck may play a more modulatory role(2,17). High-resolution imaging confirmed that active Lck
329 is enriched within the immune synapse, whereas the inactive form is excluded to the periphery,
330 reinforcing the idea that spatial compartmentalization of Lck activity is critical for signal fidelity.

331 In mice, the presence of LCK bound to CD8 is not essential for the antiviral and antitumor functions
332 of cytotoxic T cells. However, it plays a kinase-dependent role in enhancing CD8+ T cell responses to
333 weaker antigens. Conversely, LCK associated with CD4 is crucial for the proper development and
334 activity of helper T cells, primarily through a kinase-independent mechanism that stabilizes CD4 on
335 the cell surface(20). As free Lck is the primary initiator of TCR signaling(17), then the Csk preference
336 for phosphorylating free Lck suggests a built-in regulatory checkpoint. This ensures that only the right
337 spatial and temporal context allows TCR triggering, preventing spontaneous or inappropriate
338 activation. The system may keep free Lck in a controlled but restrained state (most likely in a closed
339 configuration), where it can rapidly respond to TCR engagement but is otherwise kept inactive by Csk.
340 This would allow rapid signal initiation while maintaining immune tolerance. Coreceptor-bound Lck
341 might serve more as a stabilized, less dynamic pool, possibly involved in signal amplification rather
342 than initiation. This division of labor could explain why coreceptor-bound Lck is less accessible to
343 Csk.

344 During antigen recognition at the IS, Lck remains in a sustained open conformation, supporting
345 continuous TCR signaling. This localized activation ensures that signaling is tightly focused at the site
346 of contact between the T cell and the antigen-presenting cell. In contrast, Lck outside the IS undergoes
347 only transient inactivation, suggesting a dynamic but restrained regulation across the rest of the plasma
348 membrane. This spatial compartmentalization of Lck activity likely serves to prevent unintended
349 signaling while maintaining the cell's readiness to respond to new stimuli, highlighting a finely tuned
350 mechanism of T cell activation.

351 Our data refine the current understanding of Lck regulation in resting T cells by demonstrating that
352 Csk preferentially phosphorylates free, non-coreceptor-bound Lck, while CD45 dephosphorylates not
353 only the inhibitory Y505 but also the activating Y394 residue. These findings challenge the notion of
354 a static, constitutively active Lck pool and suggest a more dynamic regulatory landscape in which Lck
355 activity is tightly controlled through spatial segregation and substrate specificity. In this context, CD45
356 emerges as a dual-function phosphatase capable of both priming and attenuating Lck activity
357 depending on its localization and substrate accessibility. CD45 is a critical regulator that maintains T
358 cells in a quiescent state and sets the threshold for TCR activation(21) . This nuanced model aligns
359 with and extends the kinetic segregation framework, emphasizing the importance of membrane
360 microdomain organization and the differential regulation of coreceptor-associated versus free Lck in
361 shaping the threshold and timing of TCR signaling.

362 Together, these findings provide new insights into the spatial and conformational regulation of Lck
363 during T cell activation. The selective internalization of inactive Lck and the preferential activation of
364 free Lck at the immune synapse represent previously unrecognized layers of regulation that may fine-

tune TCR signaling. The TqLck-V2.3 biosensor offers a powerful tool for further dissecting these dynamics in physiological and pathological contexts, including autoimmunity and immunotherapy.

Conflict of Interest

The author declare that the research was conducted in the absence of any commercial or financial relationships that could be construed as a potential conflict of interest.

Author Contributions

Conceptualization, J.C.; methodology, J.C. and B.D.;.; validation, J.C., B.D.; formal analysis, J.C. and G.S.J.; investigation, J.C., M.B. and G.S.J; resources, J.C.; data curation, J.C., B.D. and G.S.J.; writing—original draft preparation, J.C.; writing—review and editing, J.C., M.B., and G.S.J.; visualization, J.C.; supervision, J.C..; project administration J.C.; funding acquisition, J.C. All authors have read and agreed to the published version of the manuscript.

Funding

This research was funded by several intramural funds from the Institute of Biomedicine and Molecular Genetics (IBGM) through the Regional Government of Castile and Leon.

Acknowledgments

I would like to specifically thank Nicholas Gascoigne for all the materials and advice provided through the years.

Bibliography

1. Ondrej B, Valecka J, Manning J, Filipp D. The pool of preactivated Lck in the initiation of T-cell signaling: a critical re-evaluation of the Lck standby model. (2014)1–12. doi: 10.1038/icb.2014.100

2. Wei Q, Brzostek J, Sankaran S, Casas J, Hew LS-Q, Yap J, Zhao X, Wojciech L, Gascoigne NRJ. Lck bound to coreceptor is less active than free Lck. *P Natl Acad Sci Usa* (2020)201913334. doi: 10.1073/pnas.1913334117

3. Nika K, Nika K, Soldani C, Soldani C, Salek M, Salek M, Paster W, Paster W, Gray A, Gray A, et al. Constitutively Active Lck Kinase in T Cells Drives Antigen Receptor Signal Transduction. *Immunity* (2010) 32:766–777. doi: 10.1016/j.immuni.2010.05.011

395 4. Simeoni L. Lck activation: puzzling the pieces together. *Oncotarget* (2017) 8:102761–102762. doi:
396 10.18632/oncotarget.22309

397 5. Moogk D, Zhong S, Yu Z, Liadi I, Rittase W, Fang V, Dougherty J, Perez-Garcia A, Osman I, Zhu
398 C, et al. Constitutive Lck Activity Drives Sensitivity Differences between CD8+ Memory T Cell
399 Subsets. *The Journal of Immunology* (2016)1600178. doi: 10.4049/jimmunol.1600178

400 6. Ballek O, Broučková A, Manning J, Filipp D. A specific type of membrane microdomains is
401 involved in the maintenance and translocation of kinase active Lck to lipid rafts. *Immunol Lett* (2012)
402 142:64–74. doi: 10.1016/j.imlet.2012.01.001

403 7. Philipsen L, Reddycherla AV, Hartig R, Gumz J, Kästle M, Kritikos A, Poltorak MP, Prokazov Y,
404 Turbin E, Weber A, et al. De novo phosphorylation and conformational opening of the tyrosine kinase
405 Lck act in concert to initiate T cell receptor signaling. *Science signaling* (2017) 10:eaaf4736. doi:
406 10.1126/scisignal.aaf4736

407 8. Stirnweiss A, Hartig R, Gieseler S, Lindquist JA, Reichardt P, et al. T Cell Activation Results in
408 Conformational Changes in the Src Family Kinase Lck to Induce Its Activation. *Science signaling*
409 (2013) 6:ra13–ra13. doi: 10.1126/scisignal.2003607

410 9. Kästle M, Merten C, Hartig R, Kaehne T, Liaunardy-Jopeace A, Woessner NM, Schamel WW,
411 James J, Minguet S, Simeoni L, et al. Tyrosine 192 within the SH2 domain of the Src-protein tyrosine
412 kinase p56Lck regulates T-cell activation independently of Lck/CD45 interactions. *Cell Commun*
413 *Signal* (2020) 18:183. doi: 10.1186/s12964-020-00673-z

414 10. Letourneur F, Malissen B. Derivation of a T cell hybridoma variant deprived of functional T cell
415 receptor α and β chain transcripts reveals a nonfunctional α-mRNA of BW5147 origin. *Eur J Immunol*
416 (1989) 19:2269–2274. doi: 10.1002/eji.1830191214

417 11. Paster W, Paar C, Eckerstorfer P, Jakober A, Drbal K, Schütz GJ, Sonnleitner A, Stockinger H.
418 Genetically encoded Förster resonance energy transfer sensors for the conformation of the Src family
419 kinase Lck. (2009) 182:2160–2167. doi: 10.4049/jimmunol.0802639

420 12. Hoerter JAH, Brzostek J, Artyomov MN, Abel SM, Casas J, Rybakin V, Ampudia J, Lotz C,
421 Connolly JM, Chakraborty AK, et al. Coreceptor affinity for MHC defines peptide specificity
422 requirements for TCR interaction with coagonist peptide-MHC. *J Exp Med* (2013) 210:1807–1821.
423 doi: 10.1084/jem.20122528

424 13. Zhao X, Wu L-Z, Ng EKY, Leow KWS, Wei Q, Gascoigne NRJ, Brzostek J. Non-Stimulatory
425 pMHC Enhance CD8 T Cell Effector Functions by Recruiting Coreceptor-Bound Lck. *Front Immunol*
426 (2021) 12:721722. doi: 10.3389/fimmu.2021.721722

427 14. Yu YYL, Netuschil N, Lybarger L, Connolly JM, Hansen TH. Cutting Edge: Single-Chain Trimers
428 of MHC Class I Molecules Form Stable Structures That Potently Stimulate Antigen-Specific T Cells
429 and B Cells. *J Immunol* (2002) 168:3145–3149. doi: 10.4049/jimmunol.168.7.3145

430 15. Choudhuri K, Wiseman D, Brown MH, Gould K, Merwe PA van der. T-cell receptor triggering is
431 critically dependent on the dimensions of its peptide-MHC ligand. *Nature* (2005) 436:578–582. doi:
432 10.1038/nature03843

433 16. Palmowski MJ, Parker M, Choudhuri K, Chiu C, Callan MFC, Merwe PA van der, Cerundolo V,
434 Gould KG. A Single-Chain H-2Db Molecule Presenting an Influenza Virus Nucleoprotein Epitope
435 Shows Enhanced Ability at Stimulating CD8+ T Cell Responses In Vivo. *J Immunol* (2009) 182:4565–
436 4571. doi: 10.4049/jimmunol.0803893

437 17. Casas J, Brzostek J, Zarnitsyna VI, Hong J, Wei Q, Hoerter JAH, Fu G, Ampudia J, Zamoyska R,
438 Zhu C, et al. Ligand-engaged TCR is triggered by Lck not associated with CD8 coreceptor. *Nat*
439 *Commun* (2014) 5:5624. doi: 10.1038/ncomms6624

440 18. Irles C, Symons A, Michel F, Bakker TR, Merwe PA van der, Acuto O. CD45 ectodomain controls
441 interaction with GEMs and Lck activity for optimal TCR signaling. *Nat Immunol* (2003) 4:189–197.
442 doi: 10.1038/ni877

443 19. James JR, Vale RD. Biophysical mechanism of T-cell receptor triggering in a reconstituted system.
444 *Nature* (2012) 487:64–69. doi: 10.1038/nature11220

445 20. Horkova V, Drobek A, Paprckova D, Niederlova V, Prasai A, Uleri V, Glatzova D, Kraller M,
446 Cesnekova M, Janusova S, et al. Unique roles of co-receptor-bound LCK in helper and cytotoxic T
447 cells. *Nat Immunol* (2023) 24:174–185. doi: 10.1038/s41590-022-01366-0

448 21. Hui E, Vale RD. In vitro membrane reconstitution of the T-cell receptor proximal signaling
449 network. *Nature Structural & Molecular Biology* (2014) 21:133–142. doi: 10.1038/nsmb.2762

450

451

452

453

454

455

456

457

458

459

460

461

462

463

464

465

466

467

468

469

470

471 **Figures**

472

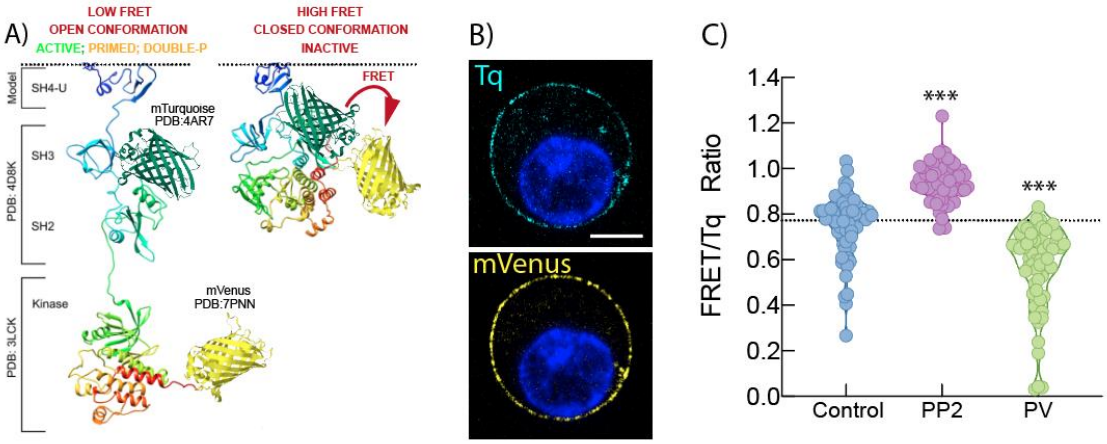

473

474 **Figure 1. Schematic representation of the conformational changes that result in FRET changes in the TqLckV2.3**
475 **biosensor.** A) The model of the open conformation (left pane) and closed conformation (right pane), modified from
476 Prakaash et al. Sci Rep (2022). B) OT-I T cell hybridoma expressing TqLckV2.3 biosensor were analyzed by confocal
477 microscopy. Scale bar, 5 µm. C) Quantitation of FRET/Tq ratio from TqLckV2.3 biosensor in OT-I T cell hybridoma
478 treated with vehicle (blue, n= 62) 10 µM PP2 Lck inhibitor (purple, n=60) or 2 min stimulation with 1 mM Pervanadate
479 (green, n=65). ***, $p < 0.001$ by Student's t test.

480

481

482

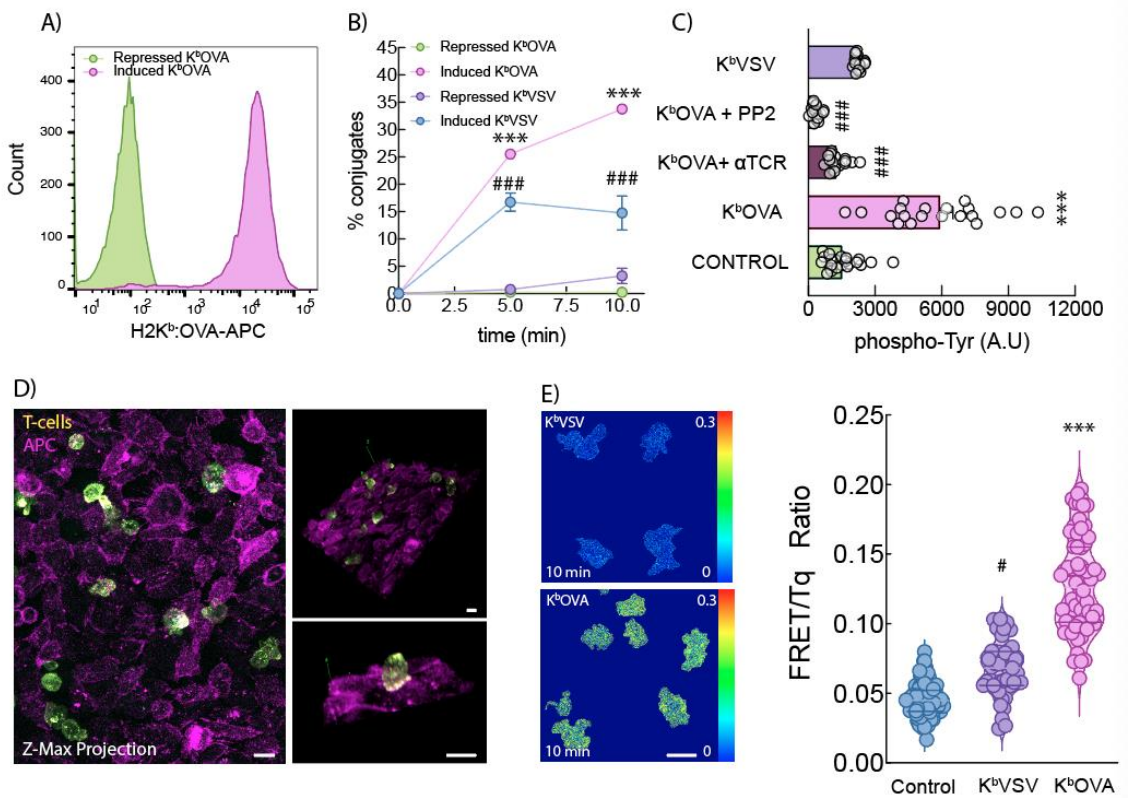

483

484

485 **Figure 2. Expression of inducible sc-MHCI agonist molecules KbOVA inCHO cells and activation of corresponding**
486 **OT-I CD8 T cells.** (A) Trex CHO cells expressing DOX-inducible sc-MHC were stained with anti-Kb:OVA and analyzed
487 by flow cytometry. Green shading: Repressed (no DOX) Trex CHO cells. Purple: Induced (+ DOX) sc-KbOVA. (B) OT-I
488 hybridomas were stimulated for the indicated times with Trex CHO cells expressing DOX-inducible sc-MHC and
489 percentage of conjugates were represented. (C) OT-I hybridomas were stimulated as in (B) for 15 min and stained with
490 anti-phospho-Tyr. Images were taken using confocal microscopy. Mean fluorescence of Control n = 23, KbOVA n = 20,
491 KbOVA + αTCR n= 18, KbOVA +PP2 n= 18 and KbVSV n = 17 ± s.e.m. is shown. (D) OT-I T cell hybridoma expressing
492 TqLckV2.3 biosensor cells were plated onto a Cy5 labeled monolayer of Trex CHO cells expressing DOX-inducible sc-
493 MHC and analyzed by confocal microscopy. A representative Z-max projection image is presented, along with two distinct
494 3D reconstructions illustrating T cell–APC interactions. E) Individual FRET/Tq ratio (representative images shown) of OT-
495 I T cell hybridoma expressing TqLckV2.3 cells. Control n = 98, KbOVA n = 65 and KbVSV n = 43.). #, $p < 0.1$; ***, $p <$
496 0.001 by Student's t test. Scale bar 5 µm.

497

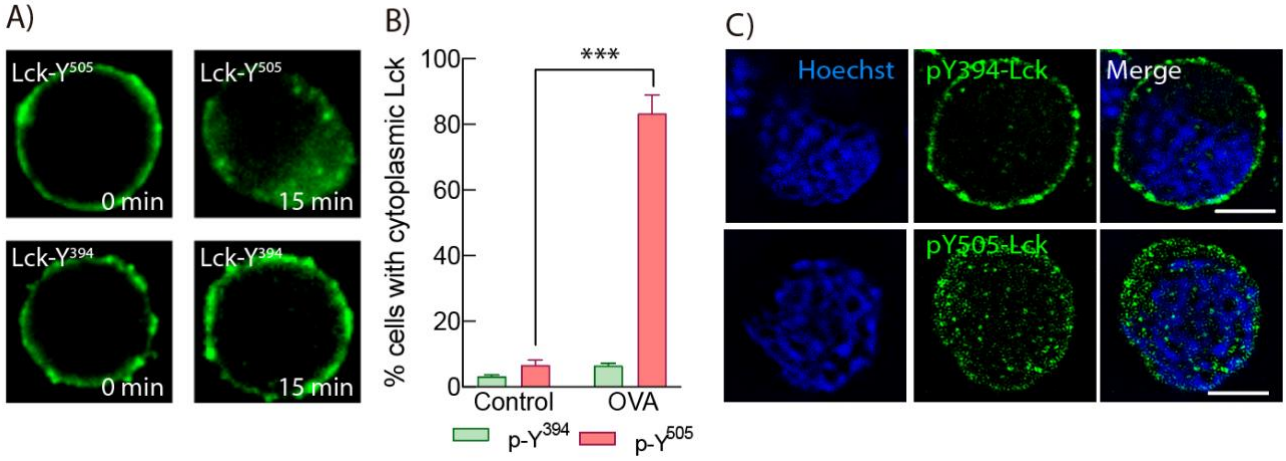

Figure 3. Spatial segregation of different phospho-Lck species. A) OT-I T cells, unstimulated and 15 min after stimulation with αCD3/CD8 crosslinking and analyzed by epifluorescecnce deconvolution microscopy B) Differential phospho-Lck antibody staining (green Y394P and red Y505P) distribution analysis from A. Bars represent % of cytoplasmic phospho-Lck ± s.e.m. >40 cells/sample. ***, $p < 0.001$ by Student's t test. C) OT-I T cells 15 min after stimulation with αCD3/CD8 crosslinking and analyzed by confocal deconvolution microscopy. Nuclei were counterstained with Hoechst 33342. Scale bar 5 μm.

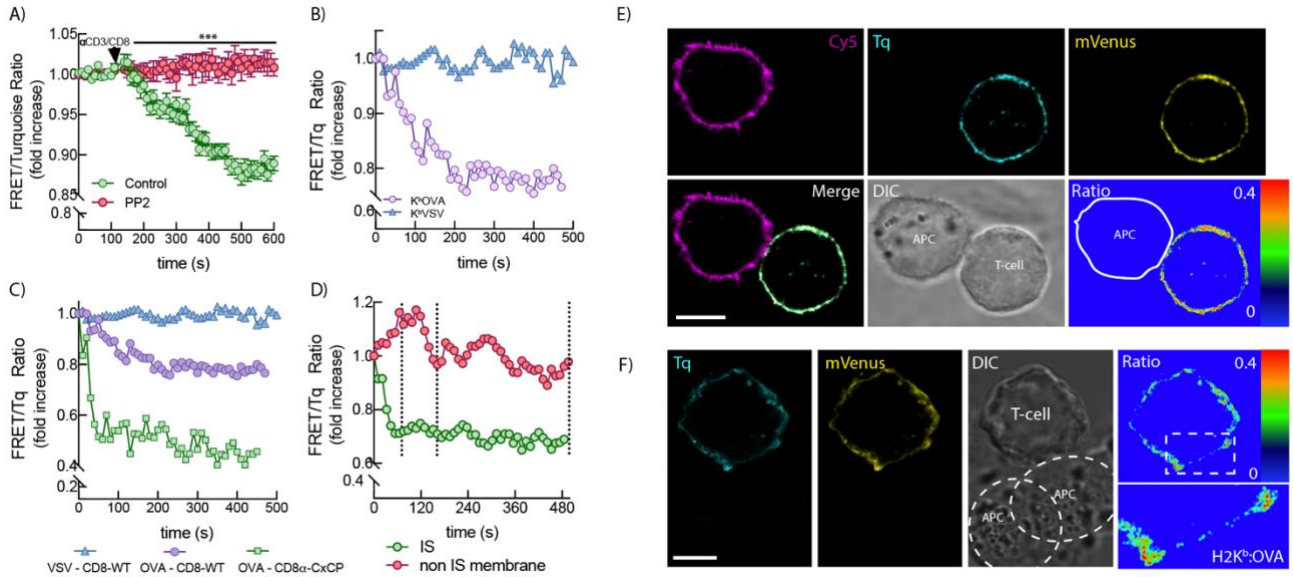

Figure 4. Lck dynamics at the Immune Synapse A) OT-I T cells expressing TqLckV2.3, untreated or pretreated with 10 mM PP2 were stimulated with αCD3/CD8 crosslinking and analyzed by live cell FRET microscopyMean FRET/Tq ratio ± s.e.m was represented. Multiple t test was applied. ***, $p < 0.001$. B) OT-I hybridomas expressing TqLckV2.3 were stimulated with Trex CHO cells expressing DOX-inducible KbOVA (purple circles) or KbVSV (blue triangles) and FRET/Tq ratio was represented since the initial contact between T cell and APC. C) Same as in B but with OT-I expressing CD8α-CxCP mutant (green squares). D) Same as in C (green circles) and rest of the plasma membrane FRET/Tq ratio analysis (red circles). The results are representative of at least three independent experiments. E) Representative image of OT-I. TqLckV2.3 expressing cells forming the immune synapse (Tq fluorescence in cyan, mVenus in yellow, CHO APC membrane labelled with Cy5 in purple and transmitted light image is shown as well) Bottom-right panel shows FRET/Tq ratio of the T cell. F) Same as in E but with unlabeled CHO. Bottom right panel shows magnification of the selected region. The results are representative of at least three independent experiments.

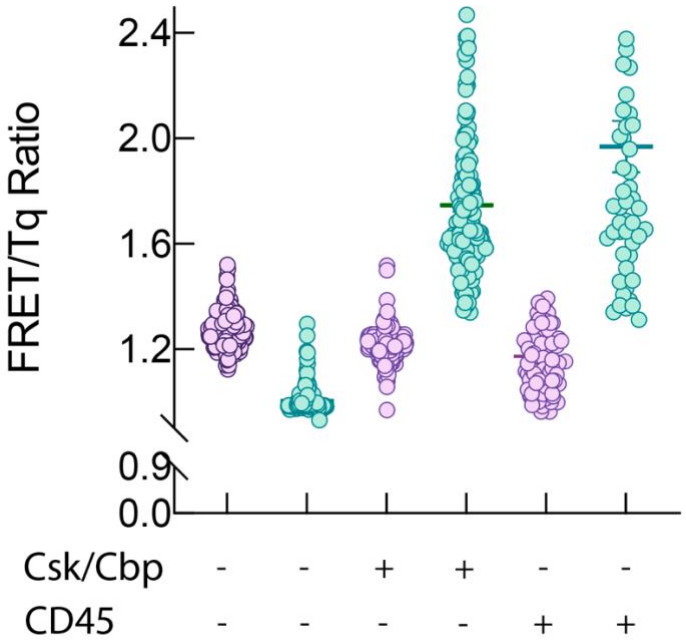

528

529

530 **Figure 5. Lck regulation in resting cells.** FRET/Tq ratio from TqLckV2.3 biosensor in unstimulated OT-I.WT (purple)
531 or OT-I.CxCP (cyan) cell hybridomas expressing Csk/Cbp or CD45cytCD43ex. WT n=233, CxCP n=139; Csk-Cbp
532 expressing WT n=262 CxCP Csk-Cbp CxCP n=149; CD45 expressing WT n=119 CD45 expressing CxCP n =52.

533